EPJ Web of Conferences **272**, 01003 (2022) https://doi.org/10.1051/epjconf/202227201003
QENS/WINS 2022

Unexpected molecular dynamics of ethanol in hydrogen-bonded binary mixtures, ethanol-octanol and ethanol-water.

Ingo Hoffmann[1,*], *Firoz* Malayil Kalathil[1,2], *Tobias* Lopian[1], *Didier* Touraud[3], *Orsolya* Czakkel[1], *Marie* Plazanet[2,**], and *Christiane* Alba-Simionesco[4]

[1]Institut Laue-Langevin, 38000 Grenoble, France
[2]Laboratoire Interdisciplinaire de Physique, CNRS and Univ. Grenoble-Alpes, 38402 Saint Martin d'Hères, France
[3]Institute of Physical and Theoretical Chemistry, University Regensburg, Universitätstraße 31, 93053 Regensburg, Germany
[4]Laboratoire Leon Brillouin, Paris-Saclay University. CEA, CNRS, 91171 Gif-sur-Yvette, France

Abstract. In view of getting a quantitative picture of the dynamics in mixtures of hydrogen-bonded liquids, in particular the ternary water-ethanol-octanol, we examine in this paper the dynamics of two binary systems: ethanol-water and ethanol-octanol. Our multiscale investigation includes quasi-elastic neutron scattering for the characterization of the dynamics at the molecular scale, completed by NMR at the mesoscopic scale and eventually compared with macroscopic viscosity properties. We highlight the decrease of diffusivity in pure alcohols when increasing the lengthscale and conjecture its relation with the two processes measured in dielectric spectroscopy. While the behaviour of ethanol-water is well understood, unexpected inversion of the slowest component between the micro and the mesoscale are evidenced in the ethanol-octanol mixture. This effect could be at the origin of the negative viscosity excess in the mixture of alcohols.

1 Introduction

Hydrogen bonded liquids, such as water and alcohols, are literally vital components of all biological systems, and essential in pharmaceuticals, food products, cryo-protection agents, microwave chemistry, and many technologically relevant materials for liquid-liquid extraction. Many important features are linked to their strong polarity that stems from the -OH dipole. Therefore, the structure of these liquids is more complicated than other organic liquids, e.g. alkanes, where van-der-Waals interactions prevail and no supramolecular structures are identified. For these systems, the local organization depends on the competition between hydrogen-bonding interactions that tend to favour clustering, and steric hindrance between alkyl chains, that limits the extension of the H-bond network. Monoalcohols, with only one donor site, can develop a two-dimensional HB network of various sizes and shapes (chains, branched chains, rings), at variance to liquid water that shows a three-dimensional HB network since the H_2O molecule has two donor and two acceptor sites.

An increased complexity is observed by mixing these liquids and the corresponding processes are widely studied in the literature because they are found in many applications over the last decades. Beside the industrial relevance of water-ethanol mixture, for example the water-octanol mixture has been studied as model system to mimic interfaces and cell membranes [1] and aggregation in the form of a reverse micelle-like or worm-like structures was suggested. Ternary aqueous mixtures also received a lot of attention as promising green solvents. The aqueous mixture of ethanol and octanol has been extensively studied during the last decade since it presents a model system for the study of the nano and meso-organization, also presenting the so-called Ouzo-effect [2], observed when an emulsion is formed after a rapid aqueous dilution of a low water content mixture, entering deeply into the two-phase region close to the binodal line. It was actually shown that a *pre-Ouzo* zone is already present in the monophasic region, extending all around the critical point (see Figure 1a for graphical visualization) [3]. This work, on the three involved binaries of this system, is a first step toward the understanding of the molecular dynamics of the pre-Ouzo region in following a line crossing the phase diagram across the region of interest.

Monoalcohols containing up to three carbon atoms are known to be fully miscible with water in any proportion. Thermodynamic excess quantities, transport properties and structure of water-ethanol mixtures as a function of mole fraction of alcohol have evidenced thermal anomalies [8, 9]. In particular, the viscosity maximum is observed for 0.25 molar fraction of ethanol, i.e., three water molecules per alcohol molecule [6]. Around this concentration, the H-bond network of water is enhanced due to the hydrophobic interaction of the ethyl groups in ethanol. Water molecules are easily added until all hydrogen bond sites of the alcohol are occupied; by adding further water, at the viscosity maximum, mesoscopic nanophase separation with water droplets is observed but the system remains macroscopically miscible. For monoalcohols containing

*e-mail: hoffmann@ill.fr
**e-mail: marie.plazanet@univ-grenoble-alpes.fr

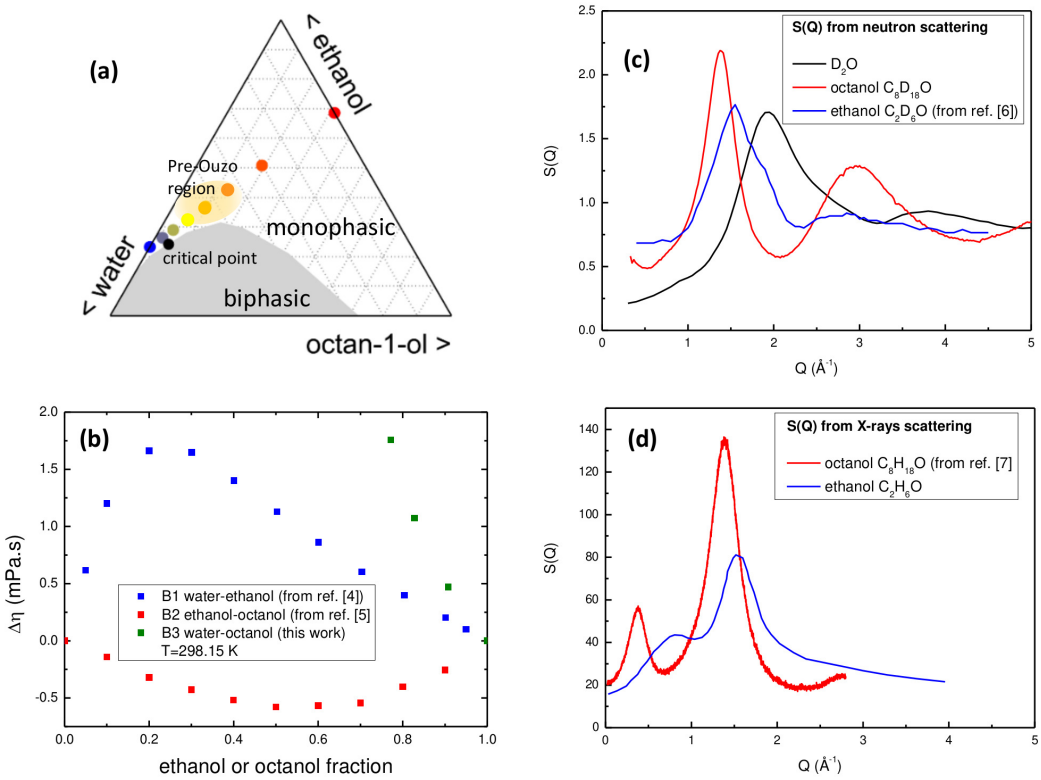

Figure 1. (a) phase diagram of the ternary mixture water-ethanol-octanol, expressed in mole fraction. The dots are distributed over the line of interest for the understanding of the ternary mixture. (b): excess viscosity for the three binary mixtures in ethanol or octanol mole fraction in their miscibility range. Data for the water-ethanol and ethanol-octanol are taken from references [4] and [5] respectively.(c) and (d) : structure factor of the pure compounds measured by neutron (our work, measurements on 7C2 at LLB, France and ref [6]) and X-ray diffraction (our work and ref. [7] respectively.

a longer alkyl chain, such as n-octanol, mixing is only possible in very limited proportions until aqueous saturation is reached: at room temperature, molar fraction solubility of water in octanol was found to be equal to 0.27 (48.91 ∓ 0.13 mg/g of water in octanol [10]). At variance to water-monoalcohol mixtures, monoalcohol mixtures, such as ethanol-octanol, exhibit a negative excess viscosity [5] (see Figure 1b), i.e., the system becomes less viscous than the ideal mixture by adding ethanol to octanol with a minimum close to a molar fraction of .5 (note that, for this latter case, one should also remember that the viscosity of monoalcohols increases with the number of carbons in the alkyl chain, ethanol being almost 8 times faster than n-octanol). Therefore, understanding the function of hydrogen-bonded liquids requires knowledge of the structure and dynamics of both the molecules and the dipoles.

The structure factor of the liquids studied in this work is reported in Figure 1 by neutron on panel (c) (our work and ref. [11]) and by X-Rays scattering on panel(d) (our work and ref. [7]). The mean peak (1-2 $Å^{-1}$) associated to intermolecular distances is shifted to higher Q's and broader for the smallest liquid, water. The occurrence of a prepeak (0-1 $Å^{-1}$), located beyond the usual short range liquid order at low wave vector is weakly seen by neutron scattering due to the low weight contribution of the O-O partial structure factor, but clearly noticeable by X-rays at room temperature for ethanol and n-octanol. Nothing equivalent is observed for water due to the smaller size of the molecule. Careful analysis of molecular dynamic simulations in terms of cluster sizes and shapes reported a fraction of ring aggregates of 27% for ethanol [11–14] and only 3.6% for octanol where chain like clusters are majority [1, 15]. The large dipole moment involved makes these associating liquids very good systems for studies by dielectric spectroscopy, a technique that has been extensively applied to this class of liquids [16–19]. It has been established for mono-alcohols, such as ethanol or octanol, and possibly water, that the dipoles relaxation occurs with a characteristic time that differ from those of the molecules. A prominent dielectric signal of Debye type appears at low frequency, i.e. with a long relaxation time slower than the relaxation of the remaining structure; it is attributed to the breaking of hydrogen bonds in molecular aggregates of 2-4-6 molecules associated in chain or ring like structures. As a result a slow mode due to the H bond network, the -OH dynamics, coexist with a faster one related to the structural relaxation and the mobility of the -OR part of the molecules.

In this framework, we investigated both binary mixtures at each end of the line crossing the ternary phase diagram, ethanol-water (B1) ethanol-octanol (B2) (0.21 and 0.65 mol fraction of ethanol in hydrogenated mixtures, re-

spectively), corresponding moreover to a constant ethanol mass fraction. We present here measurements of the diffusion coefficient at different lengthscales: at the molecular scale using Neutron Spin Echo (NSE) and at the mesoscale with NMR. Although the diffusion coefficients of pure alcohols measured with both techniques are known from the literature, we emphasize here that the characteristic timescales of the dynamics vary with the lengthscale. Using specific deuteration, we were eventually able to disentangle the diffusion coefficients of the different molecular species, exhibiting different behaviors in a macroscopically homogeneous mixture. In light of the structural organization and dynamics characterized by dielectric spectroscopy, we conjecture that the origin of the lengthscale variation of the diffusion coefficient is directly related to the mesoscale cluster organization and propose that it is also at the origin of the different signs of the excess viscosities in the various mixtures.

2 Materials and methods

Anhydrous ethanol (purity > 99.9%) and octan-1-ol (purity > 99%) were provided by Carlo Erba Reagents. Water was prepared from a Millipore source with a resistivity of 18.2 MΩcm. D_2O (99.9% D) and d6-ethanol (C_2D_5-OD, 99.0% D, <0.3% water) were obtained from Eurisotop, d17-octan-1-ol (C_8D_{17}-OH, 98% D, where only the hydroxy labile hydrogen is not deuterated) from Cambridge Isotope Laboratories. All compounds were used without further purification. All measurements presented here, including the pure ethanol and octanol but not water, were performed during the same experimental runs.

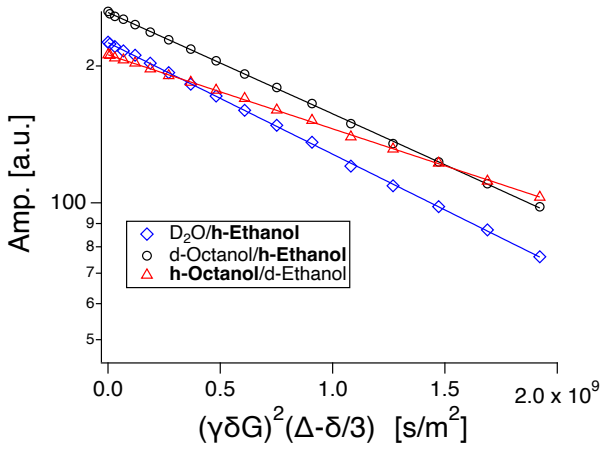

Figure 2. PFG-NMR amplitudes as a function of pulsed field gradient and fit with a single exponential function. The hydrogenated component of the binary mixture, accounting for the largest part of the signal, is in bold in the legend.

NSE measurements were performed on the instrument IN11C at a wavelength of 5.5 Å and the center of the detector positioned at an angle of 20 deg covering a Q range from 0.1 to 0.7 $Å^{-1}$ and allowing to access a maximum usable Fourier time of 1 ns. Additional NSE measurements were performed on the instrument IN15 using a wavelength of 8 Å and detector angles of 3.5, 6.5 and 9.5 deg covering a usable Q range from 0.05 to 0.145 $Å^{-1}$ and reaching maximum Fourier times of 70 ns.
Pulsed Gradient Field NMR (PGF-NMR) experiments were performed on a Bruker Minispec mq20 with a pulsed gradient unit for gradients up to 4 T/m using a standard Hahn Echo sequence with a delay between 90 and 180 deg pulse Δ=7.5 ms and a gradient pulse length δ=0.6 ms. Amplitudes vs field gradient were very well fitted using a single exponential decay, as shown in the figure 2. The lengthscale probed with NMR, equivalent of 'Q^2', is $(\Gamma\delta G)^2$. With the proton gyromagnetic ratio Γ = 26.7E7 rad/T/s, δ=0.6 ms and G from 0 to 3.2 T/m, gives Q=0.5 μm^{-1} at 3.2 T/m gradient, therefore 3 to 4 orders of magnitude larger than NSE typical lengthscale. Deuterated compounds were used in order to disentangle the different coefficients, based on the measurement of proton diffusion i.e. of the diffusion of the hydrogenated component. The extracted diffusion coefficients were therefore calculated, for each species, assuming a complete exchange of the labile hydrogen/deuterium between the hydroxyl groups. To reach this goal, two equations were coupled such as :

$$D_{meas1} = x_{11}D_1 + x_{12}D_2 \quad (1)$$

$$D_{meas2} = x_{21}D_1 + x_{22}D_2 \quad (2)$$

with x_{11} and x_{12} are the molar fraction of protons in component 1 and 2 respectively, in the measurement 1, while x_{21} and x_{22} are the molar fractions protons in component 1 and 2 respectively in the measurement 2. Equations are then inverted to extract the diffusion coefficient D_1 of the component 1 and D_2 of the component 2. This assumes that exchange of labile protons is slow compared to the time scale of the experiment and that all protons contribute equally to the NMR signal. We also neglect differences in viscosity between deuterated and hydrogenated components and we further assume 100% deuteration for the nominally deuterated components. This correction is however quite small. Results are directly presented in the section 4.
All measurements were performed at room temperature 298 K.

3 Results from NSE

Neutron Spin Echo enables the measurement of the translational diffusion coefficient on a lengthscale of a fraction of nm and a timescale smaller than a few ns. Mixtures of protonated and deuterated components were used in order to extract the dynamics of each component. Since NSE measures the difference between coherent and 1/3 of the incoherent neutron scattering signal, the data were fitted according to the equation

$$S(Q,t) = A_{coh}(Q)S_{coh}(Q,t) - A_{inc}(Q)S_{inc}(Q,t) \quad (3)$$

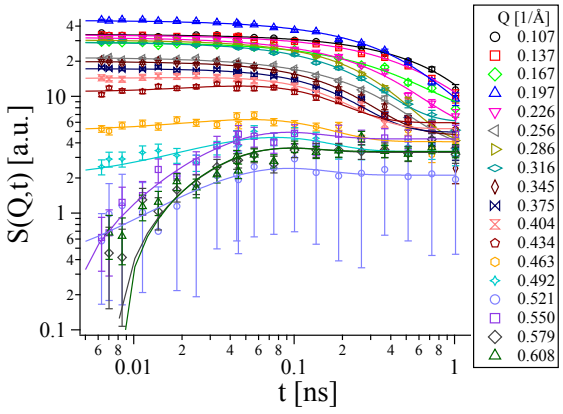

Figure 3. NSE data and fit for octanol in the B2 mixture d-ethanol/h-octanol (0.61 mol of ethanol), according to eq. 3 for the different values of Q. Data are measured on the spectrometer IN11 at the ILL (France).

where A_{coh} and A_{inc} are the (positives) coherent and incoherent amplitudes which are calculated from the polarised intensity in up and down direction assuming 100% flipper efficiency. S_{inc} is the normalised incoherent intermediate scattering function given by $S_{inc}(Q,t) = \exp(-D_{inc}Q^2t)$, where the incoherent diffusion coefficient D_{inc} is constant over the whole Q range. This last approximation therefore assumes a Fickian diffusion over the lengthscales covered by NSE, a posteriori justified by the quality of the fit. The normalised coherent intermediate scattering function S_{coh} is given by

$$S_{coh}(Q,t) = x_{inel}(Q)\exp(-\Gamma_{inel}t) + (1 - x_{inel}(Q))\left[\left(1 - x_{bkg}(Q)\right)\exp\left(-D_{coh}(Q)Q^2t\right) + x_{bkg}(Q)\right] \quad (4)$$

where D_{coh} is the Q dependent coherent diffusion coefficient, x_{bkg} is the fraction of elastic background and x_{inel} is the fraction of fast coherent dynamics [20]. Γ_{inel} has been set to a value of 300 1/ns based on the relaxation times observed in an all-deuterated sample. At this value, $\exp(-\Gamma_{inel}t)$ has essentially decayed after 8 ps. For a given Q in a given data set, we have D_{coh}, x_{bkg}, x_{inel}, in addition there is a single Q independent D_{inc} for the whole data set. The relatively large number of free parameters is eased by the fact that both x_{bkg} and x_{inel} are small corrections accounting for at most 2% of the coherent signal. The coherent (collective) dynamics is expected to be sensitive to the structural organization and therefore is allowed to vary over the investigated Q range. The IN15 data were fitted with the same model and constrained to the D_{inc} extracted from the IN11 data which covers higher Q, where the coherent signal has mostly decayed and the signal incoherent scattering is more visible. Because of the very large scattering cross section of hydrogen, we expect the incoherent signal to be dominated by the hydrogenated component. The coherent contribution is proportional to the square of the contrast, here between the hydrogenated and deuterated molecules. We assume in this analysis that the measured coherent dynamics is also the one of the hydrogenated component, justified by the good agreement between D_{coh} and D_{inc} at high Q.

Both data and fits according to eq. 3 are shown in the figure 3 for the mixture B2 where the octanol is hydrogenated. At small Q, the signal is dominated by the coherent diffusion. The incoherent contribution becomes dominant for Q larger than c.a. 0.4 Å^{-1} when the small angle intensity I(Q) drops to zero and before the structure factor increases again above 1 Å^{-1} because of to intramolecular correlations.

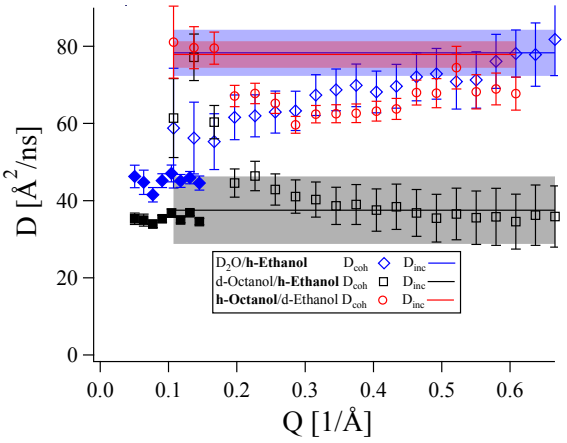

Figure 4. Coherent (empty squares) and incoherent (constant line) diffusion coefficients extracted from IN11C measurements over the whole Q range three mixtures: B1 d-water/h-ethanol, B2 d-ethanol/h-octanol, B2 h-ethanol/d-octanol, in the respective fractions of 0.14, 0.61, 0.66 mol of ethanol. Full squares are extracted from IN15 measurements. The colored zones represent the error bar on D_{inc}.

The extracted diffusion coefficients for the B1 and B2 mixtures are shown in the figure 4. D_{coh} and D_{inc}, for each sample, are quite similar and tend to agree at large Q (small distances). Deviations are observed at small Q, when probing longer distances. The collective diffusion of ethanol in the water/ethanol mixture tends to slow down over larger distances, as confirmed by the smallest Q data measured on IN15. This effect can be assigned to the presence of clusters of a few molecules as previously discussed, close to the maximum of the thermodynamic anomalies. If self and collective diffusion are similar very short distances, measuring the collective translational dynamics over larger distances (small Q) implies probing the dynamics of these aggregates. D_{coh} therefore deviates from D_{inc} and becomes slower, the diffusion of ethanol is hindered by the aggregation.

Due to the limited range of Fourier times covered by IN11C, during which barely any decay of S(Q,t) is visible at low Q, the increase of D_{coh} observed at the low Q end of the IN11C measurements for h-ethanol/d-octanol is merely an artefact as the measurements from IN15, which cover significantly longer times are clearly indicating constant values of D_{coh} at low Q. The ethanol-octanol behav-

ior will be further discussed in the next section in regards to NMR measurements.

4 Discussion

The diffusion coefficients measured by NSE and NMR of the B1 and B2 mixtures on both sides of the pre-Ouzo region are presented in figure 5. NMR probes the individual molecular diffusion similarly to incoherent QENS but over a lengthscale larger by 5 orders of magnitude. This combination enables the study of the diffusion coefficients from the nm to the micron lengthscale: a slowing down of the dynamics when the lengthscale increases is well understood in complex systems [21].

Regarding the pure compounds, water presents a dynamics characteristic time, assigned to the translational diffusion coefficient, identical for the two techniques, while diffusion of ethanol and octanol slow down with increasing lengthscale. The values presented here are in very good agreement with values reported in the literature for neutron Time-Of-Flight spectroscopy in pure water and ethanol [22, 23] and PFG-NMR for water, ethanol and octanol[24–26]. At the molecular scale, water forms a 3-D hydrogen bond network that repeats over macroscopic distances. As discussed in the introduction, clustering due to hydrogen bonding of a few molecules occurs in monoalcohols because of the presence of hydrophobic chains. Dielectric spectroscopy measurements show two relaxation times, a fast one related to internal molecular motions and a slow one related to the cluster dynamics. We conjecture that the same causes apply here: internal motions within the cluster governing the dynamics over a short lengthscale measured by neutron scattering and cluster dynamics slowing down the diffusion over larger distances. Although the Debye relaxation is also observed, to a lower extent, in pure water, we do not observe any effect of large sale structure on the diffusivity in pure water.

We then measured the diffusivity of ethanol in the water-ethanol mixture. Overall, we measure a smaller diffusivity in agreement with the increase of viscosity. When probed over the full range of NSE lengthscales corresponding to the size of a few molecules, the ethanol mixed in water exhibits a small Q dependence. However, when going up to large distances as probed by NMR, no further slowing down of the dynamics is observed : for distances larger than the ethanol clusters, the diffusivity is governed by the 3-D organization of water and the diffusivity stays constant.

Eventually, the ethanol-octanol mixture presents the most unexpected behavior. While the diffusion coefficient of octanol decreases over large distances similarly to pure octanol, the one of ethanol, at the limit of the error bars, tends to increase.

Mixtures of alcohols are known to exhibit strong negative viscosity excess. Still, the diffusivity of ethanol is lower in the mixture than in the bulk, which is not the case of octanol. On one hand, the averaged diffusivity can be calculated on the basis of the diffusion coefficients of the components in the mixture, for both NMR and NSE : $D_{av}=x_1D_{mix,1}+x_2D_{mix,2}$ were $x_{1,2}$ are the molar fractions of each component. This gives numbers of $\sim$ 57 and $\sim$ 49 10^{-11} m^2s^{-1} for NSE and NMR respectively. On the other hand, one can compute an ideal diffusivity based on the diffusion coefficients of the pure compounds : $D_{ideal}=x_1D_{bulk,1}+x_2D_{bulk,2}$. This calculation instead leads to diffusivities of $\sim$ 118 and 74 10^{-11} m^2s^{-1} respectively. Although these number indicate a negative excess of diffusivity that would lead to a positive excess of viscosity in the ethanol-octanol mixture, in opposition to its experimental value, the (absolute) diffusivity excess decreases from 60 to 25 with increasing lengthscale. A further evolution in this direction at macroscopic distances would explain the negative viscosity excess.

In this mixture, the hydrogen-bond network is not three dimensional because of the carbon chains and the larger importance of Van der Waals interactions. Ethanol is less mobile in the mixture than in the bulk at short distances but unlike the octanol, behaves more in a bulk-like way at long distances. The opposite is observed for octanol. The ethanol clusters may be hindered by the surrounding octanol molecules, but have a short enough lifetime so that the long range diffusion is less affected. Octanol molecules instead are fluidified by the presence of ethanol that locally disturbs the structural octanol organization. This last one may still persist at long distance, inducing the decrease of mobility.

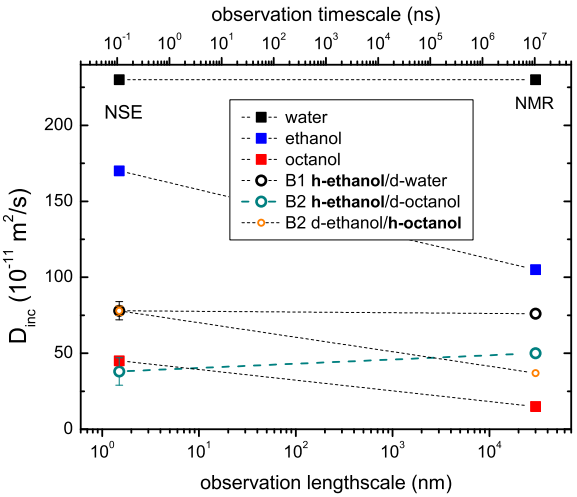

Figure 5. Self diffusion coefficients from NSE and NMR for the pure compounds and binary mixtures, measured at 298 K. In the binaries, the component characterized is in bold in the legend. Lines are only guides for the eye. Note the exceptional increase of the ethanol diffusion coefficient between NSE and NMR in the ethanol-octanol solution.

5 Conclusion and perspectives

In order to understand and rationalize the macroscopic behavior of hydrogen bonded mixtures of water and alcohols, we investigated the dynamics from the nano- to the micron scale. The use of Neutron Spin Echo in partially

deuterated mixtures enables the distinction between coherent and incoherent diffusivity, giving further insight into the molecular dynamics over the scale of small aggregates. Combined with NMR, we could characterize the diffusion coefficients of individual species in molecular mixtures on the microscopic and mesoscopic lengthscale.

We emphasize that pure alcohols already present diffusivities that slow down over long distances with respect to molecular scale. This observation is in agreement with the different relaxations observed with dielectric spectroscopy on very different observables which are the dipoles.

In the binary systems, we observe complex behaviors of the molecular dynamics, changing with distance and time in a non intuitive manner. We propose that the positive excess viscosity measured in water-alcohols mixture is related to the long range extend of the hydrogen bond network due to the dominating water dynamics. In mixtures of alcohols, instead, the viscosity excess is negative. We indeed observe a singular behavior of ethanol that was not highlighted earlier and requires further investigations to be quantitatively understood, in relation to the long distance organization.
The two binaries investigated here are the most relevant of the ternary system water-ethanol-octanol, which exhibits nanoscale structuration. We expect the dynamics characterized here to be key processes in the organization of the ternary system.

Acknowledgments

We thank the ILL for beamtime and the use of PSM laboratories. We are grateful to Sylvain Prévost, Thomas Zemb and Olivier Diat for fruitful discussions.

References

[1] J.L. MacCallum, D.P. Tieleman, Journal of the American Chemical Society **124**, 15085 (2002), pMID: 12475354, https://doi.org/10.1021/ja027422o

[2] S.A. Vitale, J.L. Katz, Langmuir **19**, 4105 (2003)

[3] T.N. Zemb, M. Klossek, T. Lopian, J. Marcus, S. Schöettl, D. Horinek, S.F. Prevost, D. Touraud, O. Diat, S. Marčelja et al., Proceedings of the National Academy of Sciences of the United States of America **113**, 4260 (2016)

[4] B. González, N. Calvar, E. Gómez, Á. Domínguez, The Journal of Chemical Thermodynamics **39**, 1578 (2007)

[5] M.A.F. Faria, R.J. Martins, M.J.E.M. Cardoso, O.E. Barcia, Journal of Chemical & Engineering Data **58**, 3405 (2013), https://doi.org/10.1021/je400630f

[6] R. Böhmer, C. Gainaru, R. Richert, Physics Reports **545**, 125 (2014), structure and dynamics of monohydroxy alcohols—Milestones towards their microscopic understanding, 100 years after Debye

[7] K.S. Vahvaselkä, R. Serimaa, M. Torkkeli, Journal of Applied Crystallography **28**, 189 (1995)

[8] P.A. Artola, A. Raihane, C. Crauste-Thibierge, D. Merlet, M. Emo, C. Alba-Simionesco, B. Rousseau, Journal of Physical Chemistry B **117**, 9718 (2013)

[9] D. Rak, M. Sedlák, The Journal of Physical Chemistry B **123**, 1365 (2019), pMID: 30532969, https://doi.org/10.1021/acs.jpcb.8b10638

[10] B.E. Lang, Journal of Chemical and Engineering Data **57**, 2221 (2012)

[11] C.J. Benmore, Y.L. Loh, The Journal of Chemical Physics **112**, 5877 (2000), https://doi.org/10.1063/1.481160

[12] A. Vrhovšek, O. Gereben, A. Jamnik, L. Pusztai, The Journal of Physical Chemistry B **115**, 13473 (2011), pMID: 21916497, https://doi.org/10.1021/jp206665w

[13] S. Pothoczki, I. Pethes, L. Pusztai, L. Temleitner, K. Ohara, I. Bakó, Journal of Physical Chemistry B **125**, 6272 (2021), 2101.12142

[14] G. Matisz, A.M. Kelterer, W.M.F. Fabian, S. Kunsági-Máté, The Journal of Physical Chemistry B **115**, 3936 (2011), pMID: 21417299, https://doi.org/10.1021/jp109950h

[15] S. Stephenson, R. Offeman, G. Robertson, W. Orts, Chemical Engineering Science **62**, 3019 (2007)

[16] T. Sato, R. Buchner, The Journal of Physical Chemistry A **108**, 5007 (2004), https://doi.org/10.1021/jp035255o

[17] A. Arbe, P. Malo de Molina, F. Alvarez, B. Frick, J. Colmenero, Phys. Rev. Lett. **117**, 185501 (2016)

[18] J.S. Hansen, A. Kisliuk, A.P. Sokolov, C. Gainaru, Phys. Rev. Lett. **116**, 237601 (2016)

[19] S.K. Garg, C.P. Smyth, The Journal of Physical Chemistry **69**, 1294 (1965), https://doi.org/10.1021/j100888a033

[20] I. Hoffmann, Frontiers in Physics **8** (2021)

[21] Q. Berrod, F. Ferdeghini, J.M. Zanotti, P. Judeinstein, D. Lairez, V. García Sakai, O. Czakkel, P. Fouquet, D. Constantin, Scientific Reports **7**, 2241 (2017)

[22] J. Qvist, H. Schober, B. Halle, The Journal of Chemical Physics **134**, 144508 (2011), https://doi.org/10.1063/1.3578472

[23] T. Seydel, R.M. Edkins, K. Edkins, Physical Chemistry Chemical Physics **21**, 9547 (2019)

[24] K.C. Pratt, W.A. Wakeham, J. Chem. Soc., Faraday Trans. 2 **73**, 997 (1977)

[25] D. Bellaire, H. Kiepfer, K. Münnemann, H. Hasse, Journal of Chemical and Engineering Data **65**, 793 (2020)

[26] M. Iwahashi, Y. Ohbu, T. Kato, Y. Suzuki, K. Yamauchi, Y. Yamaguchi, M. Muramatsu, Bulletin of the Chemical Society of Japan **59**, 3771 (1986), https://doi.org/10.1246/bcsj.59.3771